Tellus SERIES B CHEMICAL AND PHYSICAL METEOROLOGY
PUBLISHED BY THE INTERNATIONAL METEOROLOGICAL INSTITUTE IN STOCKHOLM

Tellus (2008), 60B, 657–673
Printed in Singapore. All rights reserved

TELLUS

Chemical composition of the background aerosol at two sites in southwestern and northwestern China: potential influences of regional transport

By WEN J. QU[1,2]*, XIAO Y. ZHANG[2], RICHARD ARIMOTO[3], DAN WANG[4], YA Q. WANG[2], LI W. YAN[4] and YANG LI[2,4], [1]*Key Laboratory of Physical Oceanography, Department of Marine Meteorology, College of Physical and Environmental Oceanography, Ocean University of China, 238 Songling Road, Laoshan District, Qingdao 266100, China;* [2]*Key Laboratory of Atmospheric Chemistry, Centre for Atmosphere Watch & Services (CAWAS), Chinese Academy of Metrological Sciences, China Meteorological Administration, 46 Zhong-Guan-Cun S. Ave., Beijing 100081, China;* [3]*Carlsbad Environmental Monitoring & Research Center, New Mexico State University, Carlsbad, New Mexico, USA;* [4]*State Key Laboratory of Loess and Quaternary Geology, Institute of Earth Environment, Chinese Academy of Sciences, 10 Fenghui S. Rd., PO Box 17, XiAn 710075, China*

(Manuscript received 5 February 2007; in final form 2 January 2008)

ABSTRACT

Concentrations of organic carbon (OC), elemental carbon (EC), selected trace elements and water-soluble (WS) ions were determined for samples collected from August 2004 to February 2005 to assess the aerosol background at two remote sites in China. The OC and EC concentrations in PM_{10} from near the Tibetan Plateau at Zhuzhang (ZUZ) were comparable with other background sites, averaging 3.1 and 0.34 $\mu g\ m^{-3}$, respectively, with no pronounced seasonality. At Akdala (AKD) on northern margin of the Zhungaer Basin, the average concentrations were similar (mean OC = 2.9 $\mu g\ m^{-3}$ and EC = 0.35 $\mu g\ m^{-3}$), but the concentrations were higher in winter. The aerosol mass at both sites was dominated by OC and SO_4^{2-}, but a stronger contribution from soil dust was observed at AKD. At ZUZ, NO_3^- showed a unique weather-related fluctuation in PM_{10} with a periodicity of ~1 week. Anthropogenic sources in the Sichuan Basin and southeastern Yunnan Province evidently influence ZUZ in summer and autumn while pollutants from Russia and the China–Mongolia border affect AKD nearly all year. The identification of these upwind sources demonstrates that transboundary transport needs to be taken into account when assessing air quality in remote parts of China.

1. Introduction

Atmospheric aerosols are intricately linked to the climate system and hydrologic cycle because these particles can scatter and absorb radiant energy, provide condensation nuclei for cloud formation and participate in heterogeneous chemical reactions (Kaufman et al., 2002). However, uncertainties in the magnitudes of their effects on the earth's interconnected systems are large, mainly due to limited knowledge on the aerosols' composition, optical and physical properties (including shape, form and size) and to a lack of information on their temporal and geographical distributions.

Aerosol concentrations vary strongly over time and space, and frequent measurements are required to provide realistic representations of the variability in their loadings as well as their averages. Accurate depictions of aerosol distributions are important for understanding their effects on climate and for evaluating their large-scale impacts on earth systems. Unfortunately, these kinds of data are limited, especially for remote parts of the world where information on emissions is lacking and where few observations have been made.

Studies at remote sites are often designed to provide representations of the aerosol population over a large area, thus providing information on background conditions upon which pollution events or other perturbations are superimposed. Ideally, these sites should be sufficiently far from major cities and emission sources so that their influences are minimized but with logistics suitable for making all of the necessary measurements. Because it is difficult, if not impossible, to ensure that a site is free of human disturbance, separating pollution events from baseline conditions has proven challenging. This dilemma may also partly result from ambiguity and arbitrariness with respect to

*Corresponding author.
e-mail: quwj@ouc.edu.cn; quwj@163.com
DOI: 10.1111/j.1600-0889.2008.00342.x

what constitutes background or baseline atmospheric conditions and data.

Hidy and Blanchard (2005) have discussed several terms, including natural background, background, unmanageable background and baseline levels, related to these concepts. From a survey of global data, these authors concluded that the background concentrations of fine particles and their chemical composition are highly variable, both spatially and temporally. They further note that in addition to the inevitable local anthropogenic perturbations to particle concentrations, there are regional-scale (synoptic) meteorological influences, including long-range pollutants transport events. Therefore, we want to acknowledge that while we are dealing with data for samples collected from remote background sites, a true 'natural background aerosol' is in practical terms not measurable. That is, the results reported in this paper are for the well-mixed background aerosol, with limited but inevitable influences from anthropogenic activities and regional transport.

In China, observations at regional atmospheric background sites have been made for decades, but those observations mainly targeted gaseous species, such as O_3, CO, CO_2, CH_4, SO_2 and NO_x. Similarly, observations of atmospheric aerosols at regional background sites have been mostly short term, and they have mainly involved trace elements and water-soluble (WS) ionic species (Ma et al., 2003; Wang et al., 2004). Data for carbonaceous aerosols in East Asia are particularly scarce (Hitzenberger and Tohno, 2001; Xu et al., 2002; Zhang et al., 2005). Some studies have involved observations of the radiative properties of atmospheric aerosols (Xu et al., 2002, 2003), but these observations, too, generally have been discontinuous or short in duration.

Here, we present aerosol observations made during sampling campaigns at two remote background sites in China. The first site is Zhuzhang (ZUZ), which is in a mountainous rural area of southwestern China, and the other, Akdala (AKD), is in a hilly area in the northwestern part of the country. The objectives of this study were to (1) characterize composition of aerosol particle samples from these two remote regions by determining the concentrations from mineral dust, organic carbon (OC), elemental carbon (EC), sulphate, filterable nitrate and ammonium; (2) investigate temporal variations of the aerosols and (3) investigate the transport pathways for the aerosols. We will discuss the variations and statistical distributions of selected chemical constituents to better depict the undisturbed background characteristics of the aerosols from these two regions in a subsequent paper.

2. Sampling and analysis

2.1. Sampling

Measurements of aerosol particle composition were conducted at two sites: (1) Zhuzhang (ZUZ, 28° 00′ N, 99° 43′ E, 3583 m), on the southeastern margin of the Tibetan Plateau in southwestern China and (2) Akdala (AKD, 47° 06′ N, 87° 58′ E, 562 m), in the Eerqisi Valley, which is on the northern margin of the Zhungaer Basin. Sampling was conducted from August 2004 to February 2005 at ZUZ and from July 2004 to March 2005 at AKD (Fig. 1 and Table 1). The Bay of Bengal is situated to the southwest of ZUZ and the South China Sea to the southeast, and as a result, marine air-parcels have the potential to influence the climate and composition of the atmosphere at ZUZ.

In contrast, AKD is located in northwestern China (in the centre of Eurasia), and it has an arid climate, frequently experiencing cold air incursions in winter and spring. There are extensive areas of semi-desert and desert in northwestern China, southern Mongolia and southeastern Kazakhstan around this region with

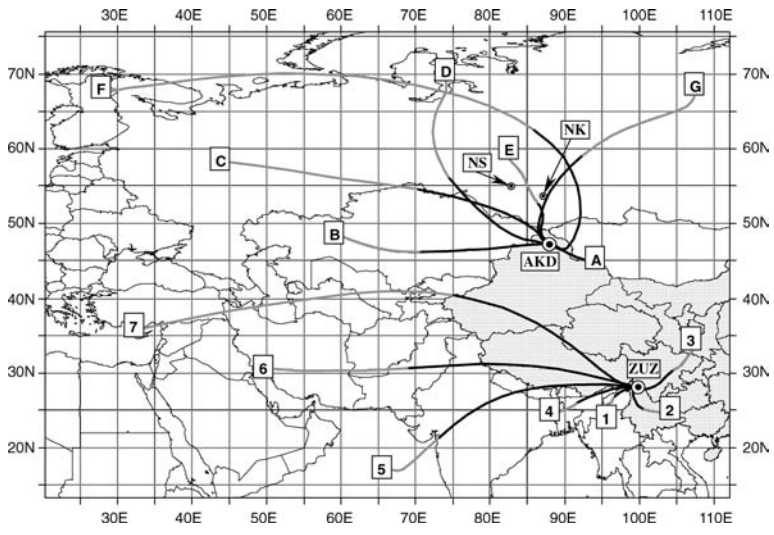

Fig. 1. Sampling sites and clusters of 5-d back trajectories for Zhuzhang (ZUZ) (Cluster 1–7) and Akdala (AKD) (Cluster A–G). The shadowed area represents continental China. NK denotes Novokuznetsk, while NS marks Novosibirsk. The average 1 to 3 day backward in time trajectories are shown as black lines, whereas the average trajectories extended 4–5 d are shown as grey lines.

Table 1. Site descriptions for the aerosol sampling during year of 2004 and 2005

Sampling station	Site description	Sampling period	Instrument and flow rate	Sampling time and height
Zhuzhang (ZUZ) (28° 00′ N, 99° 43′ E)	3583 m above the sea level; a remote China Atmosphere Watch Network (CAWNET) background station in the north of Shangri-La County (Yunnan province, China); located on the south-east margin of the Tibetan Plateau, Southwestern China.	1 August. 2004 to 28 February. 2005	TEOM® 1400a ∼15.7 L min^{-1}	74 72 hour averaged (normally from 8:00–8:00) bulk PM_{10} aerosol samples collected from a 5 m tall building
Akdala (AKD) (47° 06′ N, 87° 58′ E)	562 m above the sea level; a remote China Atmosphere Watch Network (CAWNET) background station to the south of Aletai city; situated in the Eerqisi Valley which is located on the north margin of the Zhungaer Basin, Northwestern China	26 Jul. 2004 to 10 Mar. 2005	TEOM® 1400a ∼15.7 L min^{-1} for PM_{10}, FA-40 aerosol sampler∼30 L min^{-1} for TSP	57 72 hour averaged (normally from 8:00–8:00) bulk PM_{10} aerosol samples collected from a 5 m tall building, 23 daytime averaged (normally from 8:00–20:00) bulk TSP aerosol samples from 2 m tall above ground

land cover typical of semi-desert, grassland and crops from mixed farming. The Gurbantunggut Desert is to the south of AKD, and this is an important source for Asian dust (Zhang et al., 2003a). Moreover, AKD is situated in the westerly wind regime, and dust can be transported to the site from the deserts in Kazakhstan by the prevailing winds. AKD is windy year-round. The maximum instantaneous wind velocity could reach 30 m s^{-1}. Therefore, one would expect dust to be a major contributor to the aerosol population at AKD.

Local anthropogenic emissions should have minimal impacts at ZUZ and AKD because they are both rural sites far from cities or strong residential sources. Therefore, the results we present for these sites are arguably characteristic of the well-mixed aerosol populations transported from regional or distant sources. These data can thus be viewed as indicators of background conditions.

Bulk aerosol particles were collected on 47 mm diameter Whatman quartz microfibre filters (QM/A, Whatman Ltd, Maidstone UK) that were preheated at 800 °C for 4 hour to remove contaminants before use. 47 mm diameter Teflon™ (PTFE) filters (WTP, Whatman Ltd, Maidstone UK) were used for the first week sampling at ZUZ and for the first two weeks sampling at AKD (Table 1). These Teflon™ filter samples were only used for the analysis of major ions and trace elements. The PM_{10} and total suspended particle (TSP) masses were determined gravimetrically with the use of an electronic microbalance with 1 μg sensitivity (ME 5-F, Sartorius AG, Goettingen Germany). After sampling, the aerosol-laden filters were stored in petri dishes which were enclosed in plastic bags and when necessary they were refrigerated at 4 °C before chemical analysis.

2.2. Determination of OC and EC

The bulk samples were analysed directly for OC/EC using a DRI Model 2001 Thermal/Optical Carbon Analyser following the IMPROVE thermal/optical reflectance (TOR) procedure (Chow and Watson, 2002). The OC/EC analyses were conducted at the Key Laboratory of Atmospheric Chemistry, Centre for Atmosphere Watch and Services (CAWAS), Chinese Academy of Metrological Sciences in Beijing. For the analyses, a 0.526 cm^2 circular punch prepared from a sample filter was heated stepwise at temperatures of 120 °C (which yields the OC1 fraction), 250 °C (OC2), 450 °C (OC3) and 550 °C (OC4) in a non-oxidizing (He) atmosphere, and at 550 °C (EC1), 700 °C (EC2) and 800 °C (EC3) in an oxidizing atmosphere (2% oxygen and 98% He). The carbon that evolved at each temperature was oxidized to carbon dioxide (CO_2), and then reduced to methane (CH_4) for quantification with a flame ionization detector.

As the temperature increases in the instrument's helium atmosphere, some of the organic carbon pyrolyzes, forming black carbon; this results in the darkening of the filter deposit. This conversion process is monitored by measuring the reflectance of light produced with a He–Ne laser at a wavelength of 633 nm. When oxygen is added to the atmosphere, the residual organic and pyrolysed black carbon combust, and the reflectance increases. The amount of carbon measured after oxygen is added

until the reflectance returns to its original value is reported as optically detected pyrolyzed carbon (OPC).

While eight fractions (OC1, OC2, OC3, OC4, EC1, EC2, EC3 and OPC) can be reported separately, the IMPROVE protocol defines OC as OC1+OC2+OC3+OC4+OPC and EC as EC1+EC2+EC3-OPC. Volatile organic carbon (VOC) denotes organic carbon that evolved from the filter punch in the He-only atmosphere at 120 °C during analysis, that is, the first organic carbon peak, which was likely present mainly as volatiles (Non-methane hydrocarbons, NMHC). The OC/EC analyser was calibrated with known quantities of CH_4 each day of operation. Replicate analyses were performed at the rate of once per group of 10 samples. The difference determined from replicate analyses was <7% for TC (total carbon), and <10% for OC and EC. All data were corrected for backgrounds from the average of three blank filters (0.68 OC μg cm^{-2}; 0.01 EC μg cm^{-2}) for the ZUZ samples and three different blank filters (0.44 OC μg cm^{-2}; 0.01 EC μg cm^{-2}) for the AKD samples.

Table 2. The average masses of the elements in PM_{10} samples and the average blank values of the prepared quartz microfibre filters at ZUZ

	Arithmetic mean ± standard deviation		
	Average masses in PM_{10} samples	Average blank values	Detection limit[a]
S (μg/filter)	14 ± 6.9	5.4 ± 0.39	1.2
Ca (μg/filter)	52 ± 2.6	48 ± 0.49	1.5
Fe (μg/filter)	4.1 ± 2.0	2.4 ± 0.069	0.21
K (μg/filter)	10 ± 1.5	8.1 ± 0.26	0.77
Ti (μg/filter)	0.93 ± 0.28	0.65 ± 0.026	0.077
Mn (μg/filter)	0.28 ± 0.45	0.084 ± 0.013	0.038
Pb (μg/filter)	0.23 ± 0.16	0.14 ± 0.003	0.009
As (μg/filter)	0.097 ± 0.064	0.022 ± 0.011	0.033

[a]Determined as three times of the standard deviation of the blank values.

2.3. Determination of water-soluble (WS) ionic species

Chemical analyses of the WS ionic species, including SO_4^{2-}, NO_3^-, NH_4^+, Ca^{2+}, Mg^{2+}, K^+, Na^+, NO_2^-, Cl^- and F^-, were conducted for the bulk samples collected on both Whatman quartz fibre filters and Teflon™ filters with the use of a Dionex 600 ion chromatograph (IC) equipped with an electrochemical detector (Dionex ED50A). One quarter of each 47 mm filter sample was extracted with 10 ml double-deionized water (DDI, with a specific resistance ≥18.2 MΩ cm^{-1}) in sealed Falcon™ polypropylene centrifuge tubes, while the Teflon™ filter sample was pre-wetted with 100 μl ethanol before extraction. The filters and extraction solutions were sonicated four times (15 min each time) with 15 min of cooling in between to prevent ammonium volatilization that otherwise would have resulted from the warming of the solution due to the ultrasonic treatment. The aqueous extracts were filtered using 0.45 μm syringe filters and when necessary stored in a refrigerator at 4 °C prior to analysis.

A Dionex IonPac® AS11-HC anion-exchange column (4 mm) with an AG11-HC guard column and an ASRS® ULTRAII self-regenerating anion suppressor (4 mm) were used for the anion analyses; the eluent for anion analysis was 25 mM KOH delivered at a flow rate of 1.0 ml/min. For cation determinations, a Dionex IonPac® CS12A cation-exchange column (4 mm) with a CG12A guard column and a CSRS® ULTRAII self-regenerating cation suppressor (4 mm) were used with an eluent of 20 mM methane sulfonic acid (MSA) pumped at a flow rate of 1.0 ml/min. The injection volume was 100 μl for both anion and cation analyses.

The quantifiable limits (QL) in ng m^{-3} (determined as three times of the standard deviation of the measured values for blank filters) were 3.6 for SO_4^{2-}, 0.2 for NO_3^-, 0.1 for NH_4^+, 1.2 for Ca^{2+}, 0.5 for Mg^{2+}, 0.2 for K^+, 1.2 for Na^+, 0.01 for NO_2^-, 0.6 for Cl^- and 0.2 for F^-. It is important to note that the measured nitrate includes both aerosol nitrate and nitric acid sorbed to the filters, and therefore it has been referred to as 'filterable nitrate' (Arimoto et al., 2004a). The uncertainties for all the WS ionic species, which demonstrate the reproducibility of the analysis, were all less than 3.5%: 0.6% for SO_4^{2-}, 0.5% for NO_3^-, 1.1% for NH_4^+, 2.6% for Ca^{2+}, 1.4% for Mg^{2+}, 1.8% for K^+, 0.8% for Na^+, 3.2% for NO_2^-, 0.5% for Cl^- and 1.4% for F^-. Replicate analyses were performed once per group of 10 samples. The concentrations of these analytes in the samples are markedly higher than their QLs, and all data were corrected for backgrounds from blank filters.

2.4. Determination of trace element concentrations

Portions of the bulk samples were also analysed for trace elements directly using a proton-induced x-ray emission (PIXE) method. The PIXE analyses were performed using the 2.5 MeV protons with a 50 nA beam current produced by 2 × 1.7 MV tandem accelerator (for details see Zhang et al., 1993). The concentrations of 22 elements were determined through these procedures, including As, Br, Ca, Cl, Cr, Cu, Fe, K, Mn, Ni, Pb, S, Se, Sr, Ti, V, Zn, Zr for quartz filters and an additional four elements (Al, Mg, P, Si) for Teflon™ filters. The PIXE trace element data were all corrected for backgrounds from blank filters (randomly chosen filters subjected to shipping and gravimetric measurements in the laboratory in the same way as other filters, but without exposure and sampling procedure in the field). We note that there were consistently high blank values for K, Ca, Ti and Fe in the quartz fibre filters (Table 2). Nevertheless, the average mass concentrations of all of the elements we report in Table 2 exceeded their detection limits, which were defined as three times the standard deviations of the blank values.

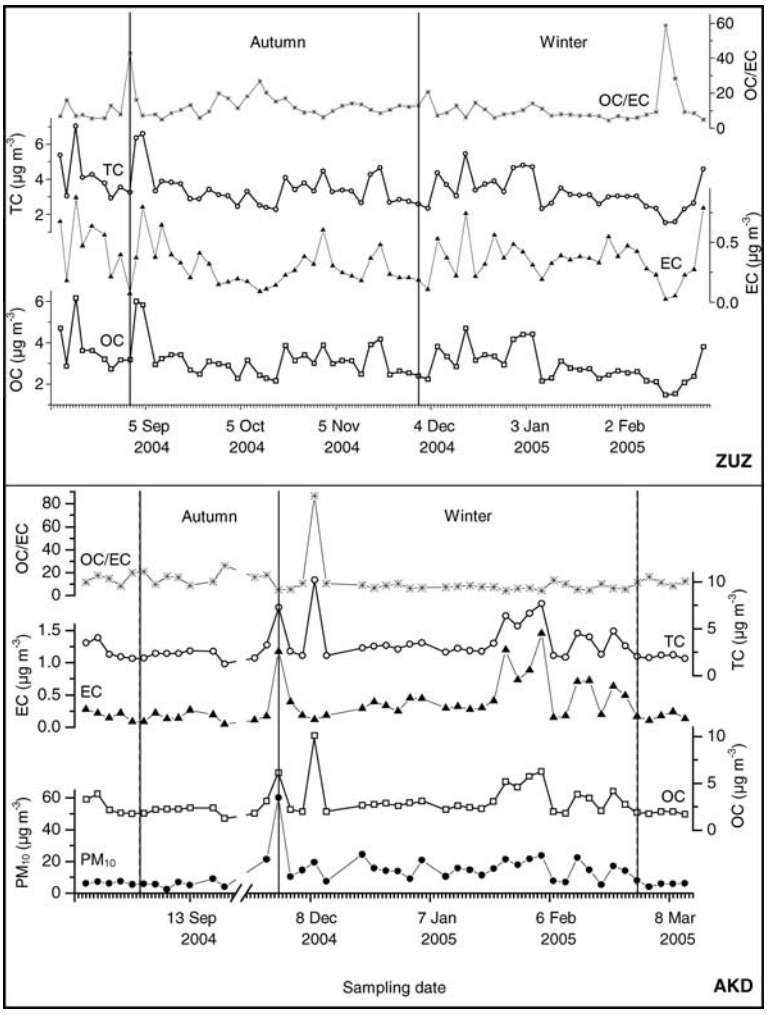

Fig. 2. Time series of organic carbon (OC), elemental carbon (EC), total carbon (TC) concentrations and OC/EC ratio in PM_{10} at ZUZ and AKD for August 2004 to March 2005.

3. Results and discussion

3.1. Time series of OC and EC, WS ionic species, and trace elements at ZUZ and AKD

3.1.1. OC and EC. At ZUZ, the EC and TC (TC, the sum of EC plus OC) concentrations in PM_{10} generally exhibited synchronous variations at low levels. Neither the OC nor the EC concentrations varied strongly with season. The OC loadings did decrease slightly from summer and autumn to winter (Fig. 2, Table 3): the arithmetic mean OC concentrations ($\pm$ standard deviation in μg m^{-3}) in August, in autumn, in winter and for the whole sampling period were 3.7 $\pm$ 1.0, 3.2 $\pm$ 0.88, 2.9 $\pm$ 0.82 and 3.1 $\pm$ 0.91, respectively. The corresponding mean EC concentrations (μg m^{-3}) were 0.45 $\pm$ 0.25, 0.30 $\pm$ 0.16, 0.36 $\pm$ 0.17 and 0.34 $\pm$ 0.18. Thus, EC was at relatively high levels in August followed by the lowest mean concentration in autumn, and then it increased slightly in winter, as was the case for SO_4^{2-} (Figs. 2 and 5, Table 3). Relatively high levels of EC and SO_4^{2-} in August likely result from material transport from Sichuan Basin and eastern Yunnan Province in summer (see Section 3.3.1). In contrast, slight increases in their concentrations during winter probably reflected enhanced regional emissions from combustion sources.

Changes in VOC emissions (Fig. 3) and the efficiency of secondary organic carbon (SOC) formation likely were at least partially responsible for the observed trends in OC. A decreasing trend of VOC concentrations in PM_{10} from summer to winter (and in its proportion of TC: 19% in summer vs. 3.0% in winter, Fig. 3) at ZUZ suggested a significant contribution of biogenic VOCs to the OC pool. This is most likely due to seasonality in the growth cycles of vegetation. Research on carbonaceous aerosol at Cheju Island, Korea, has also confirmed important influences of biogenic OC at that background site in summer (Kim et al., 2000). In addition, the formation of SOC was likely more efficient in summer and autumn when warm temperatures and strong solar radiation favoured photochemical activity that would lead to the formation of secondary aerosol particles (Dusek, 2000). The lack of strong seasonal variations in the aerosol populations

Table 3. Observed concentrations of OC, EC, WS ionic species and selected trace elements in PM_{10} during summer–winter, 2004 at ZUZ

	Arithmetic mean concentration ± standard deviation (EF_{crust}[a])			
	Aug, 2004 ($n = 13$)	Autumn, 2004 ($n = 31$)	Winter, 2004 ($n = 30$)	Aug, 2004 to Feb, 2005 ($n = 74$)
OC ($\mu g\ m^{-3}$)	3.7 ± 1.0	3.2 ± 0.88	2.9 ± 0.82	3.1 ± 0.91
EC ($\mu g\ m^{-3}$)	0.45 ± 0.25	0.30 ± 0.16	0.36 ± 0.17	0.34 ± 0.18
Na^+ ($\mu g\ m^{-3}$)	0.58 ± 0.41	0.69 ± 0.34	0.72 ± 0.28	0.68 ± 0.33
$NH4^+$ ($\mu g\ m^{-3}$)	0.18 ± 0.22	0.083 ± 0.074	0.20 ± 0.13	0.15 ± 0.14
K^+ ($\mu g\ m^{-3}$)	0.070 ± 0.043	0.060 ± 0.036	0.11 ± 0.04	0.082 ± 0.046
Ca^{2+} ($\mu g\ m^{-3}$)	0.65 ± 0.43	0.48 ± 0.23	0.42 ± 0.17	0.49 ± 0.27
$SO4^{2-}$ ($\mu g\ m^{-3}$)	1.8 ± 1.2	1.4 ± 0.68	1.7 ± 0.54	1.6 ± 0.77
$NO3^-$ ($\mu g\ m^{-3}$)	0.39 ± 0.33	0.51 ± 0.44	0.42 ± 0.20	0.45 ± 0.34
S ($\mu g\ m^{-3}$)	0.38 ± 0.38 (nd[b])	0.15 ± 0.14 (nd)	0.19 ± 0.08 (nd)	0.21 ± 0.21 (nd)
Ca ($\mu g\ m^{-3}$)	0.11 ± 0.06 (2.8)	0.13 ± 0.07 (5.5)	0.082 ± 0.044 (2.0)	0.11 ± 0.06 (3.2)
K ($\mu g\ m^{-3}$)	0.053 ± 0.042 (1.5)	0.029 ± 0.025 (1.3)	0.058 ± 0.031 (1.5)	0.045 ± 0.034 (1.5)
Fe ($\mu g\ m^{-3}$)	0.044 ± 0.029	0.027 ± 0.022	0.049 ± 0.056	0.039 ± 0.041
Pb ($ng\ m^{-3}$)	8.5 ± 8.0 (343)	2.2 ± 2.1 (140)	3.3 ± 3.3 (117)	3.9 ± 5.1 (177)
As ($ng\ m^{-3}$)	3.8 ± 3.7 (2027)	1.8 ± 1.5 (1577)	1.7 ± 1.3 (817)	2.2 ± 2.2 (1294)

[a]$EF_{crust} = (element/Fe)_{air}/(element/Fe)_{crust}$; [b]no data.

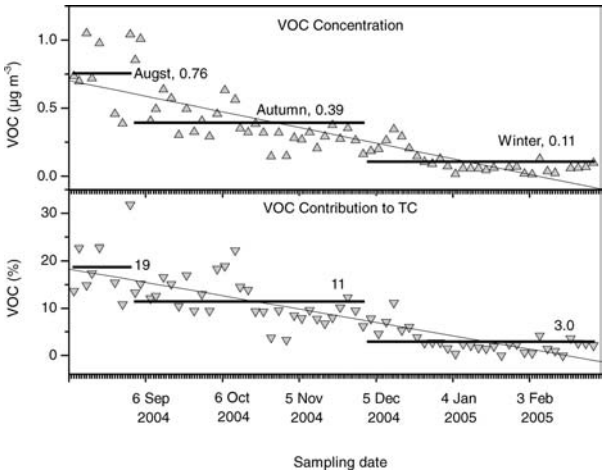

Fig. 3. Time series of volatile organic carbon (VOC) concentration and VOC contribution percentages to total carbon (TC) in PM_{10} at ZUZ for August 2004 to February 2005.

at ZUZ probably resulted from mixing upwind, but this contention needs to be verified through further observations and studies.

At AKD, the mean OC and EC PM_{10} concentrations from 16 August 2004 to 12 March 2005 were 2.9 ± 1.6 and 0.35 ± 0.31 $\mu g\ m^{-3}$. In contrast to the lack of seasonality at ZUZ, both OC and EC had distinct seasonal variations at AKD with significantly higher concentrations in winter than in other seasons (Fig. 2, Table 4). This can be explained by the long-range transport of combustion products associated with domestic heating during the long, cold winter in the region. Emissions from regional residential and biomass burning are likely sources for the carbonaceous aerosol particles (Cao et al., 2006).

3.1.2. WS ionic species.

3.1.2.1. Zhuzhang. Ion balance calculations were used to evaluate the internal consistency of the data and to determine whether significant quantities of undetected ions were present in the samples (Jain et al., 2000). Procedures used for the ion balance calculations were described in detail in Zhang et al. (2002). The ion balance evaluations for PM_{10} at ZUZ suggest an excess of cations. The ratio of anion to cation equivalents at ZUZ was ~0.6 (Fig. 4), similar to that determined for summer aerosols in nearby Lhasa, Tibet (Tang et al., 2005). Related studies have shown the presence of weak organic acids, such as formate and acetate, in the precipitation and fog-water from remote areas, especially mountainous areas such as ZUZ (Dai, 1997).

The concentrations of formate and acetate were not measured in our studies, and neither were the concentrations of CO_3^{2-} and HCO_3^-. If these anions were measured and included in the ion balance evaluations, the imbalance between the cations and anions would likely have decreased, and the internal data consistency would have improved commensurately. In any case, our evaluation of the IC data for ZUZ suggests an imbalance among measured species, and it is possible if not likely that the 'missing' anion equivalents are due to the presence of organic acids, bicarbonate and carbonate.

Time series plots of WS ions at ZUZ show that the concentrations of SO_4^{2-}, NH_4^+ and K^+ varied synchronously with various

Table 4. Observed concentrations of OC, EC, WS ionic species and selected trace elements in PM_{10} during summer, 2004 to spring, 2005 at AKD

	PM_{10}, Arithmetic mean concentration ± standard deviation (EF_{crust}[a])								
	Jul, 2004 ($n = 2$)	Aug, 2004 ($n = 12$)	Jul & Aug, 2004 ($n = 14$)	Sep, 2004 ($n = 7$)	Nov, 2004 ($n = 3$)	Sep & Nov, 2004 ($n = 10$)	Winter, 2004 ($n = 27$)	Mar, 2005 ($n = 6$)	Jul, 2004 – Mar, 2005 ($n = 57$)
OC ($\mu g\ m^{-3}$)		2.5 ± 0.83		2.0 ± 0.39	3.6 ± 1.8	2.5 ± 1.3	3.3 ± 1.8	1.8 ± 0.13	2.9 ± 1.6
EC ($\mu g\ m^{-3}$)		0.19 ± 0.07		0.15 ± 0.07	0.48 ± 0.49	0.25 ± 0.31	0.45 ± 0.32	0.16 ± 0.05	0.35 ± 0.31
Na^+ ($\mu g\ m^{-3}$)	0.063 ± 0.025	0.28 ± 0.23	0.25 ± 0.23	0.50 ± 0.09	0.60 ± 0.30	0.53 ± 0.19	0.53 ± 0.12	0.47 ± 0.07	0.46 ± 0.20
NH_4^+ ($\mu g\ m^{-3}$)	0.55 ± 0.06	0.27 ± 0.15	0.32 ± 0.17	0.085 ± 0.071	0.40 ± 0.30	0.19 ± 0.24	0.88 ± 0.34	0.50 ± 0.28	0.60 ± 0.41
K^+ ($\mu g\ m^{-3}$)	0.096 ± 0.023	0.093 ± 0.049	0.094 ± 0.046	0.077 ± 0.032	0.11 ± 0.08	0.087 ± 0.052	0.12 ± 0.05	0.047 ± 0.025	0.10 ± 0.05
Ca^{2+} ($\mu g\ m^{-3}$)	0.31 ± 0.21	0.15 ± 0.10	0.17 ± 0.14	0.22 ± 0.17	0.99 ± 0.65	0.45 ± 0.52	0.91 ± 1.4	0.36 ± 0.16	0.59 ± 1.0
$SO4^{2-}$ ($\mu g\ m^{-3}$)	2.4 ± 0.37	1.4 ± 0.40	1.5 ± 0.54	1.5 ± 0.52	3.0 ± 2.0	1.9 ± 1.4	4.8 ± 1.8	2.4 ± 1.5	3.3 ± 2.1
$NO3^-$ ($\mu g\ m^{-3}$)	0.24 ± 0.06	0.22 ± 0.25	0.23 ± 0.14	0.25 ± 0.14	1.2 ± 1.0	0.53 ± 0.71	0.79 ± 0.26	0.53 ± 0.26	0.58 ± 0.44
S ($\mu g\ m^{-3}$)	0.83 ± 0.01 (nd[b])	0.43 ± 0.26 (nd)		0.15 ± 0.03 (nd)					
Ca ($\mu g\ m^{-3}$)	0.13 ± 0.05 (1.3)	0.25 ± 0.13 (1.4)		0.15 ± 0.09 (1.3)					
K ($\mu g\ m^{-3}$)	0.14 ± 0.04 (1.6)	0.15 ± 0.06 (0.9)		0.086 ± 0.023 (0.8)					
Fe ($\mu g\ m^{-3}$)	0.11 ± 0.04	0.21 ± 0.10		0.14 ± 0.05					
Pb ($ng\ m^{-3}$)	9.2 ± 3.0 (143)	9.7 ± 5.8 (80)		5.1 ± 0.10 (66)					
As ($ng\ m^{-3}$)	1.8 ± 1.8 (375)	5.8 ± 5.9 (644)		1.1 ± 0.13 (182)					

[a]$EF_{crust} = (element/Fe)_{air}/(element/Fe)_{crust}$; [b]no data.

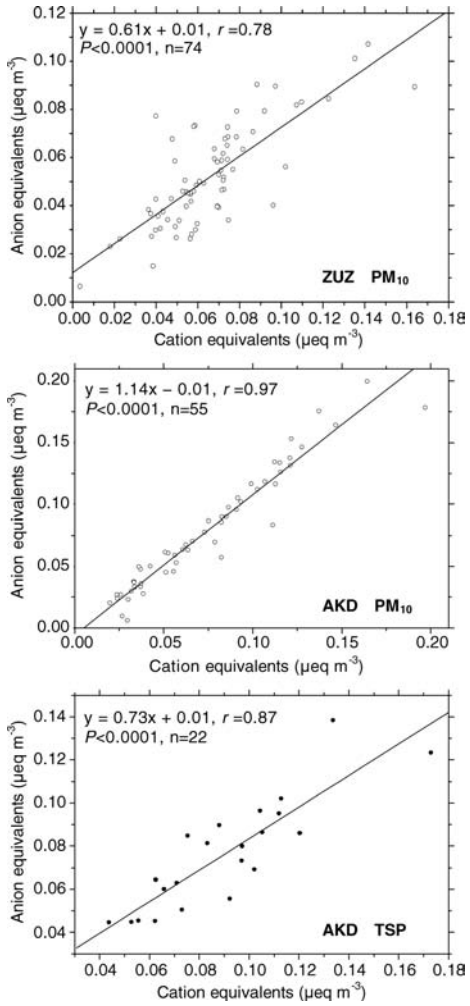

Fig. 4. Ion balance evaluation between water soluble (WS) cations and anions in PM_{10} and TSP at ZUZ and AKD.

other ions, including Ca^{2+}, Mg^{2+}, Na^+, Cl^- and NO_3^-, but not with NO_2^- or F^- (Fig. 5). The concentrations of the WS ions were comparatively low, and their variations among seasons were not pronounced (Fig. 5, Table 3). The latter presumably reflects characteristics of the background air, especially the effects of mixing upwind, and the dilution of pollutants during transport to the site.

Unique among the ions in PM_{10}, NO_3^- appeared to vary with weather conditions, with an average of 0.55 μg m^{-3} on sunny and partly cloudy days to 0.36 μg m^{-3} on rainy and cloudy days at ZUZ. The periodicity of these fluctuations was about 1 week (Figs. 5 and 6), and this is consistent with the changes that might be expected from mesoscale weather patterns. Furthermore, the changes in filterable NO_3^- presumably reflect the influence of weather on the photochemical transformation of NO_x and formation of NO_3^-. Research by Song et al. (2005) has similarly found that the concentration of NO_2 in Beijing displayed a strong temporal variation with a quasi 5-day period, and those changes, too, have been linked to weather.

Situated on the Tibet Plateau, intensive solar radiation and high temperatures favour NO_x photochemical transformation at ZUZ on sunny days. In contrast, on rainy and cloudy days, photochemistry is less effective and wet scavenging is enhanced, and this may further contribute to the apparent response of NO_3^- to changes in weather. Such weather-related variations in nitrogen oxides may be particularly amenable to study in remote regions like ZUZ because of the limited influences from anthropogenic sources. The average NO_3^- concentrations for different weather conditions given in the preceding paragraph support this inference, and it would not be surprising if the filterable nitrate concentrations were affected by weather-related conditions, such as ambient humidity, temperature and solar radiation. Nevertheless, we suggest further validation of the fluctuating NO_3^- levels is needed in view of the complexity of sampling the semi-volatile nitrate species.

3.1.2.2. Akdala. Ion balance evaluations of WS ions at AKD showed different results for PM_{10} compared with TSP. That is, the measured anion equivalents were greater than the cation equivalents in PM_{10} but the opposite was true for TSP (Fig. 4), thus implying major differences in the ionic constituents as a function of particle size. Alkaline dust is commonly present as coarse particles in samples collected from the dust source regions; this would explain the relatively high concentrations of dust-derived, WS cations such as Ca^{2+}, Mg^{2+} and Na^+ in TSP. Related studies by Noguchi and Hara (2004) suggest that HCO_3^- in Asian dust can result in apparent ionic imbalances, especially in dust source regions because this ion typically has not been measured. Therefore the 'missing' anion equivalents in TSP at AKD likely relate to the unmeasured HCO_3^- and CO_3^{2-} in the samples, which are components of the dust usually presented as coarse particles in source regions.

In contrast, secondary aerosols containing sulphate, nitrate and ammonium mainly occur as fine particles, and this may well explain the excess anions in PM_{10}. Studies of the aerosol ions size distributions in samples from Hungary, for example, have confirmed that ammonium, sulphate, nitrate and organic acids are usually present in fine (diameter, d < 2 μm) particles, while K^+ and Cl^- had more even distributions between the fine and coarse (d > 2 μm) modes and Na^+, Mg^{2+}, Ca^{2+} and carbonate were predominantly in coarse particles (Krivácsy and Molnár, 1998). On this basis, the differences in ion imbalances apparent for PM_{10} and TSP are consistent with the expected size distributions of major cations and anions.

Summary data for WS ionic species in PM_{10} and in TSP at AKD are presented in Tables 4 and 5. Temporal variations of WS ions in PM_{10} at this site were similar, especially the trends in SO_4^{2-}, NH_4^+ and K^+ (Fig. 5, Table 4). The concentrations of SO_4^{2-} and NO_3^{2-} in PM_{10} during November and winter were significantly higher than in other months as was the case for OC and EC. This seasonality is probably related to increased

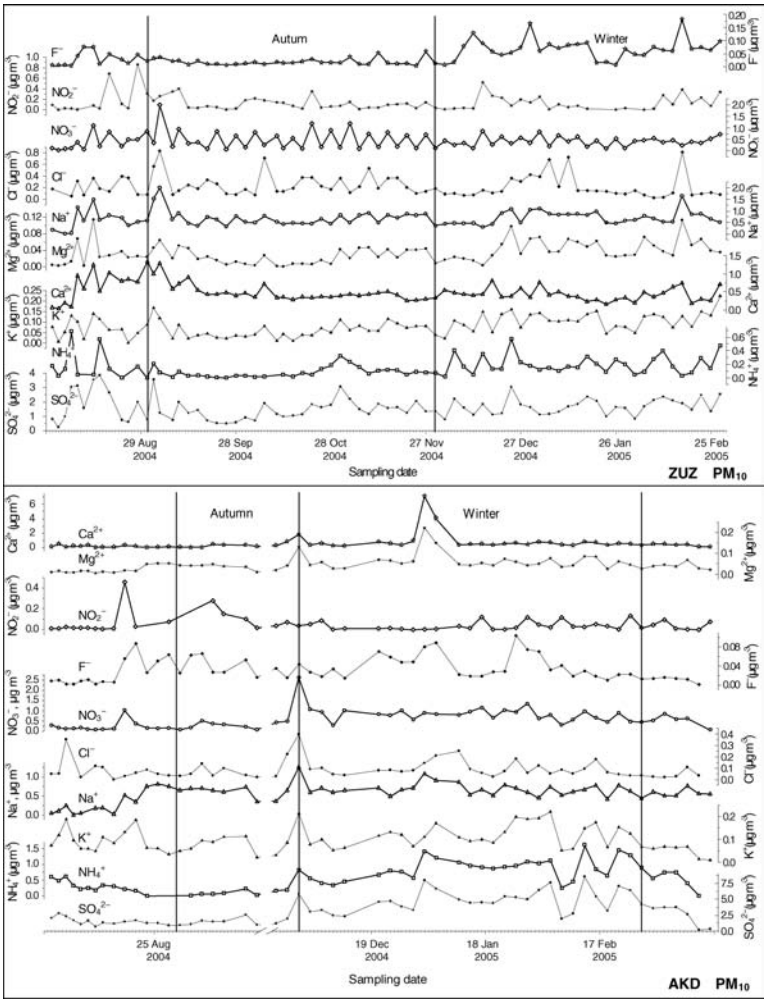

Fig. 5. Time series of water soluble (WS) ionic species in PM_{10} at ZUZ and AKD for August 2004 to March 2005.

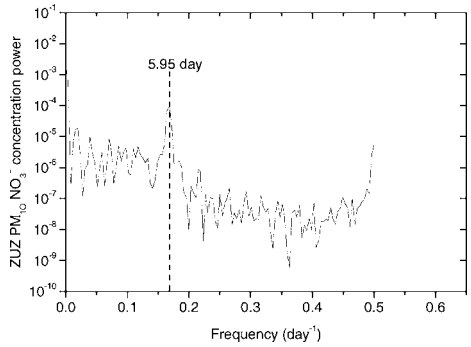

Fig. 6. Power spectrum analysis of the time series of ionic NO_3^- concentrations in PM_{10} at ZUZ for August 2004 to February 2005.

regional emissions from coal-combustion, biomass burning and other sources of energy used for domestic heating in northern Xinjiang Province and neighbouring areas.

3.1.3. Trace elements. Time series plots of the trace element concentrations at ZUZ from August 2004 to February 2005 show strong co-variations among a group of elements typically associated with crustal material, including Ca, K, Fe and Ti (Fig. 7). The mean concentrations of selected elements in PM_{10} and their enrichment factors calculated relative to crustal rock ($EF_{crust} = [Element/Fe]_{air}/[Element/Fe]_{crust}$) using the upper continental crust composition compiled by Taylor and McLennan, 1995) are summarized in Table 3. Elemental Ca, K, Fe, Ti, Si, Al and Mg had EF_{crust} values less than 5, consistent with their presumed crustal origin, but EF_{crust} values significantly larger than 5 for Zn, Zr, Pb, As, Ni, Se, V, Cu, Cr and P show that there also were influences from non-crustal, likely pollution sources.

Time series plots of the trace elements concentrations in PM_{10} from AKD for July to September 2004 show co-variation of the following: Ca, Fe, K, Ti, Al, Mn and Sr (Fig. 8). The concentrations and EF_{crust} values for this group of elements in PM_{10} and TSP are summarized in Tables 4 and 5 (sampling of PM_{10} and TSP were not synchronous). EF_{crust} values for Ca, K, Fe, Mn, Ti, Sr, Si, Al and Mg were all close to unity, with maximum values less than 5, and this is consistent with a crustal origin for these elements. In contrast, Zn, Pb, As, Ni, Cu and Cr were influenced

Table 5. Observed concentrations of OC, EC, WS ionic species and selected trace elements in TSP during summer–autumn, 2004 at AKD

	TSP, Arithmetic mean concentration ± standard deviation (EF_{crust}[a])				
	Jul, 2004 ($n = 2$)	Aug, 2004 ($n = 12$)	Jul & Aug, 2004 ($n = 9$)	Sep, 2004 ($n = 23$)	Jul–Sep, 2004 ($n = 14$)
OC ($\mu g\ m^{-3}$)	7.5 ± 0.64	4.4 ± 1.4	4.9 ± 1.7	3.7 ± 0.7	4.4 ± 1.5
EC ($\mu g\ m^{-3}$)	0.55 ± 0.01	0.40 ± 0.17	0.42 ± 0.17	0.32 ± 0.16	0.38 ± 0.17
Na^+ ($\mu g\ m^{-3}$)	0.71 ± 0.07	0.49 ± 0.22	0.52 ± 0.22	0.94 ± 0.45	0.69 ± 0.39
$NH4^+$ ($\mu g\ m^{-3}$)	0.36 ± 0.04	0.21 ± 0.15	0.24 ± 0.15	0.075 ± 0.091	0.17 ± 0.15
K^+ ($\mu g\ m^{-3}$)	0.088 ± 0.018	0.099 ± 0.043	0.098 ± 0.040	0.15 ± 0.07	0.12 ± 0.06
Ca^{2+} ($\mu g\ m^{-3}$)	0.98 ± 0.12	0.97 ± 0.37	0.97 ± 0.34	0.68 ± 0.38	0.85 ± 0.39
$SO4^{2-}$ ($\mu g\ m^{-3}$)	2.3 ± 0.37	1.9 ± 0.75	2.0 ± 0.72	2.1 ± 0.87	2.0 ± 0.79
$NO3^-$ ($\mu g\ m^{-3}$)	0.99 ± 0.27	0.86 ± 0.34	0.88 ± 0.33	0.79 ± 0.16	0.84 ± 0.28
S ($\mu g\ m^{-3}$)	0.27 ± 0.03 (nd [b])	0.25 ± 0.11 (nd)		0.28 ± 0.12 (nd)	0.26 ± 0.11 (nd)
Ca ($\mu g\ m^{-3}$)	0.28 ± 0.20 (0.9)	0.46 ± 0.22 (1.2)		0.49 ± 0.30 (1.3)	0.45 ± 0.26 (1.2)
K ($\mu g\ m^{-3}$)	0.18 ± 0.09 (0.7)	0.26 ± 0.10 (0.7)		0.26 ± 0.13 (0.7)	0.25 ± 0.12 (0.7)
Fe ($\mu g\ m^{-3}$)	0.34 ± 0.17	0.46 ± 0.20		0.44 ± 0.27	0.44 ± 0.23
Pb ($ng\ m^{-3}$)	nd	6.3 ± 5.2 (24)		11 ± 9.8 (45)	7.4 ± 6.9 (29)
As ($ng\ m^{-3}$)	0.29 ± 0.00 (20)	5.0 ± 7.6 (253)		2.1 ± 1.5 (113)	3.5 ± 5.8 (186)

[a]$EF_{crust} = (element/Fe)_{air}/(element/Fe)_{crust}$; [b]no data.

by non-crustal sources with EF_{crust} values larger than 5. Furthermore, the enrichments were always larger in PM_{10} than in TSP, showing that the non-crustal material was mainly present in the smaller particle size fraction.

3.2. Mass balance of atmospheric aerosols for ZUZ and AKD

The mass contributions of the main types of aerosol particles, including carbonaceous material (OC and EC), sulphate, nitrate, ammonium and soil dust and associated species were calculated to evaluate their contributions to the aerosol population. One can estimate the soil dust (dust entrained into the atmosphere from surface soil) fraction of the bulk aerosol based on the 4% elemental Fe content of the Asian dust. This value was determined for Asian dust samples collected from a site on the southern margin of the Mu Us Desert (Zhang et al., 2003b), and it is similar to average values for the earth's upper continental crust. 'Other species' simply denotes the aerosol mass not accounted for in Fig. 9. It should also be noted that because measurement of the trace elements in PM_{10} was only conducted for July–September 2004 at AKD, the fraction denoted 'soil dust and other species' at AKD was estimated by taking the difference between PM_{10} mass loading and sum of the measured species for the entire sampling period.

OC was the most abundant component of the aerosol population at ZUZ (accounting for 47% of PM_{10} mass) followed by SO_4^{2-} and soil dust (24% and 13%, respectively), EC accounted for about 5.1% of the measured mass. At AKD, SO_4^{2-} contributed the greatest amount of the aerosol mass (34% of PM_{10}), while OC and EC contributed about 29% and 3.5%, respectively; soil dust and other species, which was mostly soil dust, at least during the period for which the elemental data were available, contributed about 21% (Fig. 9).

Thus, OC and SO_4^{2-} dominated the aerosol mass at both sites, but soil dust contributed more to the mass at AKD (Fig. 9). A significantly higher proportion of OC in the aerosol mass at ZUZ relative to AKD may have resulted from differences in the primary sources of biogenic VOCs as well as from the more efficient formation of secondary carbonaceous particles. However, a higher contribution from sulphate to the aerosol mass at AKD was probably a consequence of more emissions from coal combustion in the region and neighbouring areas, especially in winter; moreover, regional transport of industrial pollutants may more strongly influence air quality at this site (see Section 3.3.2).

3.3. Transport pathways

Back trajectory analysis has become a powerful tool for establishing the spatial domain of air parcels arriving at receptor sites. Five-day air mass backward in time trajectories, generated with the NOAA HYSPLIT4 trajectory model (Draxler and Hess, 1998) were used to investigate the source regions of the particles and to evaluate transport to the sampling sites. The end points for the trajectories at both ZUZ and AKD were set to 1000 m above surface; this height was chosen because the influence of the complex topography at both sites extends to relatively high altitudes. The trajectories were calculated from the NCEP (National Center for Environmental Prediction) FNL (final analysis) meteorological data fields, and they were calculated four times each day (00, 06, 12 and 18 UTC).

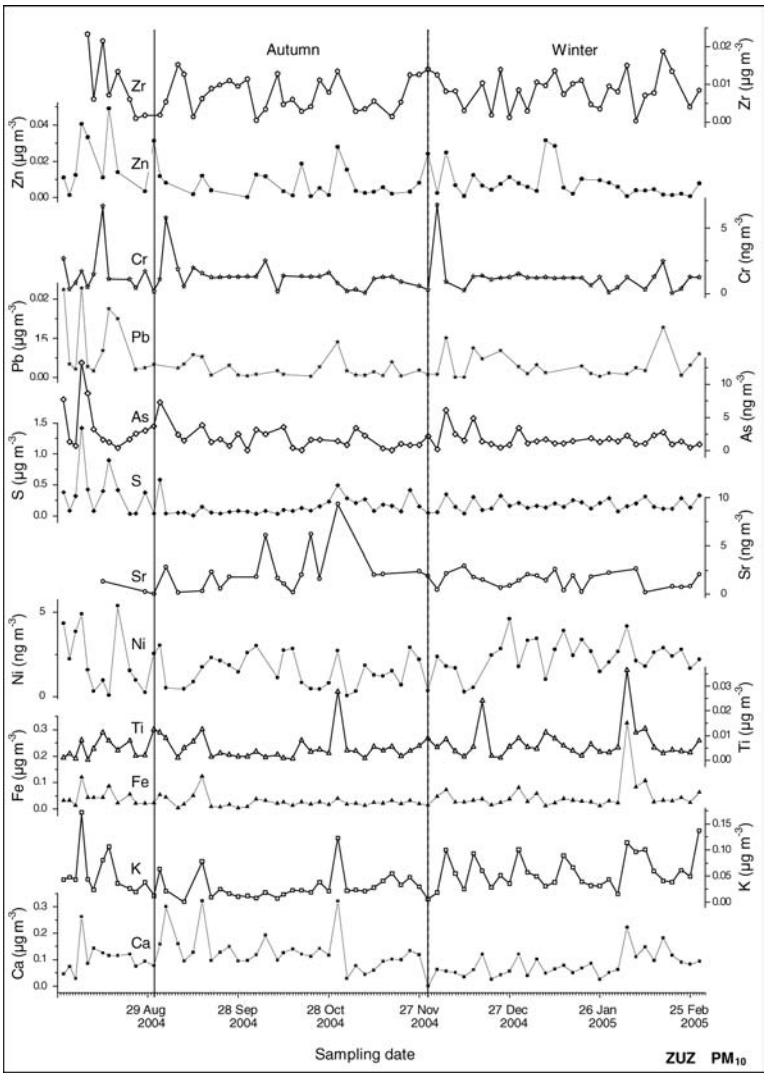

Fig. 7. Time series of trace elements in PM_{10} at ZUZ for August 2004 to February 2005.

Trajectory clustering analysis, a multivariate statistical analysis method, was used to divide the trajectories into distinct transport clusters (Moody and Galloway, 1988; Arimoto et al., 1999). In this method, squared Euclidean distances were used to determine the similarities between the trajectories, and Ward's method was used to make hierarchical clusters of the trajectories. The numbers of clusters chosen for discussion were subjectively determined by comparing the differences among the mean trajectories. The trajectory clusters are not discussed in numerical or alphabetical sequence here simply because they are labelled based on the results of the clustering procedure; they are, however, arranged in a generally counterclockwise direction (Fig. 1). Individual 5-d backwards-in-time trajectories for the clusters at ZUZ and AKD are presented to better illustrate the actual transport of the aerosols in Figs. 10 and 11.

It should be noted that the 4- to 5-d back trajectories (marked with grey lines in Fig. 1) likely have large associated uncertainties, especially for AKD where the circulation is complex and the trajectories pass over areas with scant meteorological coverage. We might also note that errors of 20% of the distance travelled seem to be typical for trajectories computed from analysed wind fields (Stohl, 1998). With this concern regarding uncertainties noted, we would argue that the backward trajectory clustering approach provides one of the best available means for investigating the source regions of the air that was sampled, especially the 1–3 d trajectory clusters (black lines in Fig. 1).

3.3.1. Transport pathways to Zhuzhang. The transport pathways to ZUZ can be classified into three types (Figs. 1 and 10, Table 6), and in general, strong seasonal variations in the transport pathways to ZUZ were evident. First, the pathways responsible for the transport of pollution were most common in summer and autumn, and these included the northeasterly trajectories (Cluster 3, C-3) from the Sichuan Basin where there are extensive emissions from coal-combustion and mining and the southeasterly trajectories (C-2) which passed over southeastern Yunnan Province. Grouping the concentration data by clusters

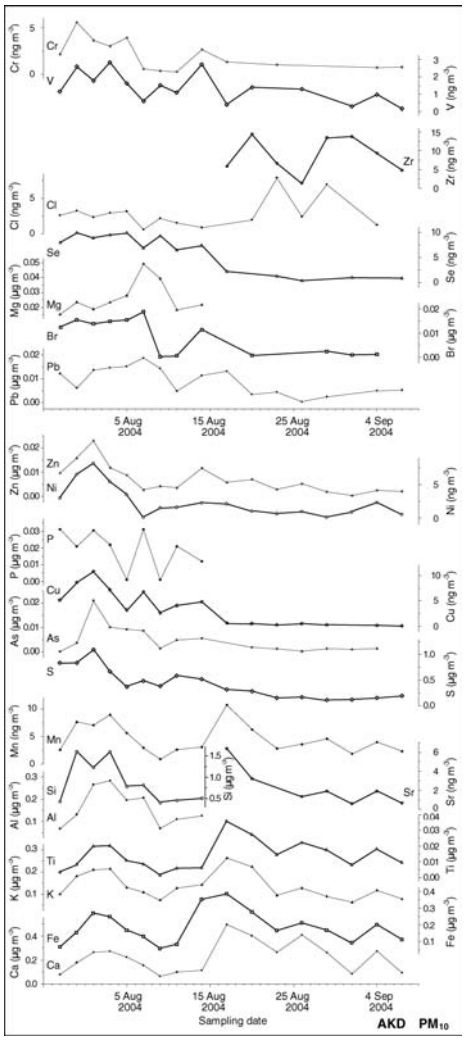

Fig. 8. Time series of trace elements in PM_{10} at AKD for July to September 2004.

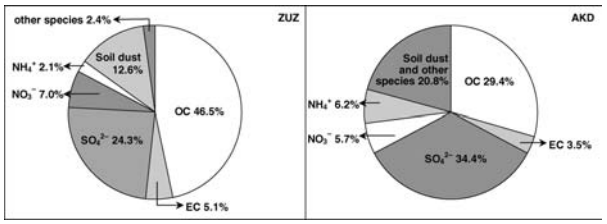

Fig. 9. Aerosol mass balances for PM_{10} at ZUZ and AKD.

shows that the highest loadings of SO_4^{2-}, which was the dominant WS ion in many samples, were associated with these two clusters. Both EC and NH_4^+ had their highest concentrations for C-3 (northeasterly trajectories), and the trace elements' concentrations, too, generally were high for the southeasterly and northeasterly trajectories.

The second set of trajectory clusters includes the southwesterly pathways from coastal regions near the Bay of Bengal (C-1 and C-4), which essentially track the transport of moisture carried by the south-west monsoon. These trajectories are typically accompanied by precipitation, and the loadings of aerosol species in this second set of trajectories were comparatively low, presumably due at least in part to wet scavenging (Table 6). The third group of clusters is represented by the remote southwesterly pathways from the Arabian Sea in South Asia (C-5) and the remote westerly and northwesterly pathways from West Asia and East Europe (C-6 and C-7). These trajectories most often occurred in autumn and winter, and they were from remote regions with relatively low-pollutant burdens.

In Table 6, one finds that the highest concentrations of OC and EC were in clusters C-2, C-3 and C-5 (southeasterly, northeasterly and remote southwesterly pathways). VOCs showed obvious seasonal variations. That is, the highest VOC concentrations were in clusters C-2 and C-3 (southeasterly and northeasterly trajectories), which only occurred in summer and autumn. The southwesterly trajectories (C-1), which mainly occurred in summer and autumn also had a comparatively high VOC values. Interestingly, the VOC concentrations were the lowest for C-5 (remote southwesterly trajectories), which only occurred in winter. This may imply VOCs are affected more strongly by seasonal changes in vegetative cover and ambient temperature rather than by shifts in regional transport pathways.

Many WS ions, including Na^+, K^+, Mg^{2+}, F^-, Cl^- and NO_3^-, had their highest concentrations in samples from the cluster of remote southwesterly trajectories from the Arabian Sea (C-5). Moreover, the concentrations of Na^+, F^- and Cl^- were relatively high for the southwesterly and southeasterly trajectories (C-1, C-4 and C-2), that is, when transport was from coastal regions, especially as compared with the low concentrations of these ions for C-3 (northeasterly trajectories) from the interior of China. The combination of chemical and trajectory results suggest that these ions probably were from sea-salt aerosols.

On the other hand, elemental Ca and WS Ca^{2+} can be used as indicators of mineral dust in aerosol samples (Arimoto et al., 2004b). At ZUZ, the mean Ca^{2+} concentrations were similar for all of the trajectory clusters other than C-1 and C-2, which covered short-distances and had the highest levels of Ca^{2+}. The concentrations of elemental Ca also tended to be higher for the samples with short-distance trajectories (Clusters 1–4, 111 ng m^{-3} to 138 ng m^{-3}) compared with the long-range transport pathways (Clusters 5–7, 72 ng m^{-3} to 95 ng m^{-3}). These results suggest a stronger contribution from nearby dust sources compared with regional dust transport.

The efficient mixing upwind and limited local anthropogenic influences were a likely reason for the limited seasonality observed in the aerosol populations at ZUZ. The mixtures of aerosols there remained relatively similar throughout the year despite the fact that the transport pathways to the site clearly changed with season (Table 6). Therefore, air sampled

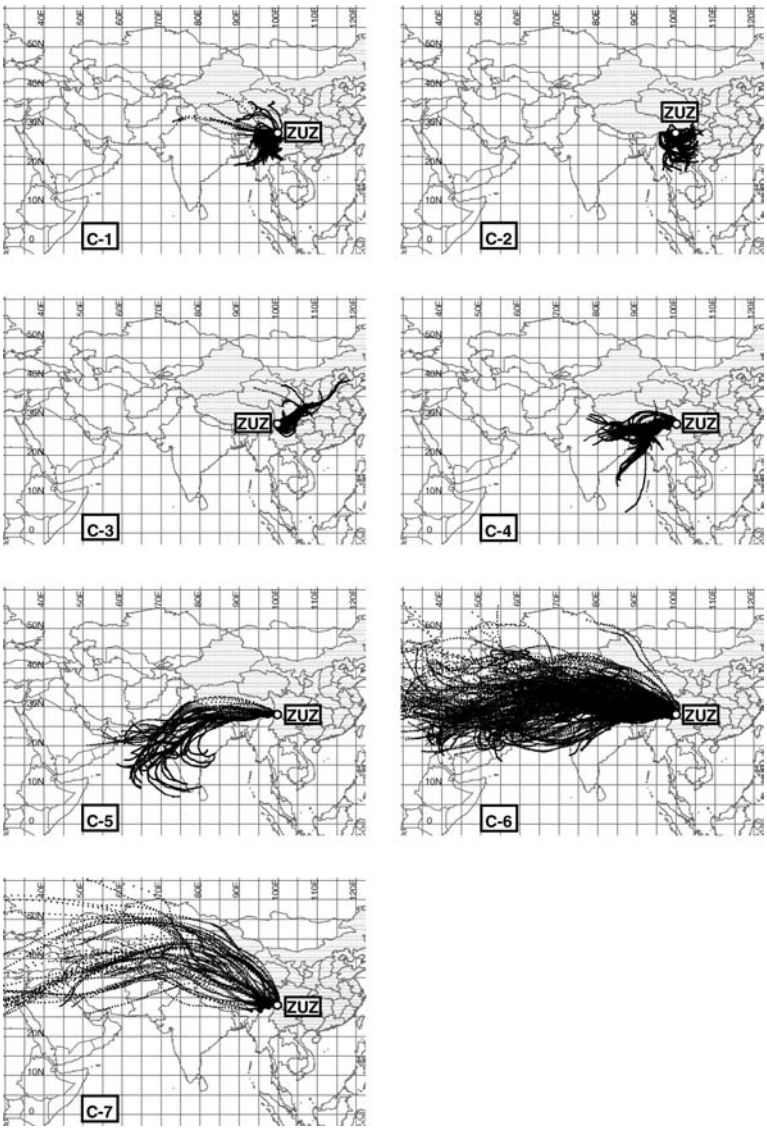

Fig. 10. Individual 5-d backwards-in-time trajectories for clusters 1–7 (C-1–7) terminating at ZUZ. The interval between the adjacent points for each trajectory is 1 hour. The shadowed area represents continental China.

at ZUZ appears to be broadly representative of regional conditions.

Indeed, geographical patterns showed that the transport pathways to ZUZ can pass over Yunnan, Sichuan, Guizhou, Chongqing and Tibet in southwestern China as well as over South Asian countries, such as India, Burma, Bangladesh and Nepal. From these results, one can infer that the levels of pollution at ZUZ approach those representing regional background conditions in southwestern China and that this background is influenced by the transport of pollutants from South Asian countries.

3.3.2. Transport pathways to Akdala. Transport to AKD is mainly controlled by the westerly wind regime, and therefore, the main sources for the aerosols lie to the west and northwest of the site. As TSP sampling and measurement of the trace elements was only conducted for a limited period at this site, the discussion of transport to AKD is based on the results of OC/EC and WS ions in PM_{10}.

Three main types of transport pathways to AKD were identified (Figs. 1 and 11, Table 6). First, the northeasterly, northwesterly and southeasterly trajectories (Clusters C-G, C-E and C-A, respectively) apparently were the major transport pathways for air pollutants because PM_{10}, OC, EC, SO_4^{2-}, NO_3^-, NH_4^+, K^+ and F^- generally had high concentrations in samples from these clusters. The C-G (northeasterly) trajectories, which appear to be the most seriously polluted, arrive at AKD after passing near Novokuznetsk (NK, population 565 000), a major industrial city in central Russia where steel production, metallurgy and coal mining are major potential sources of emissions. The C-E (northwesterly) trajectories also pass close to NK and Novosibirsk (NS, population 1 426 000), the third largest city in Russia and the largest in Siberia where the major

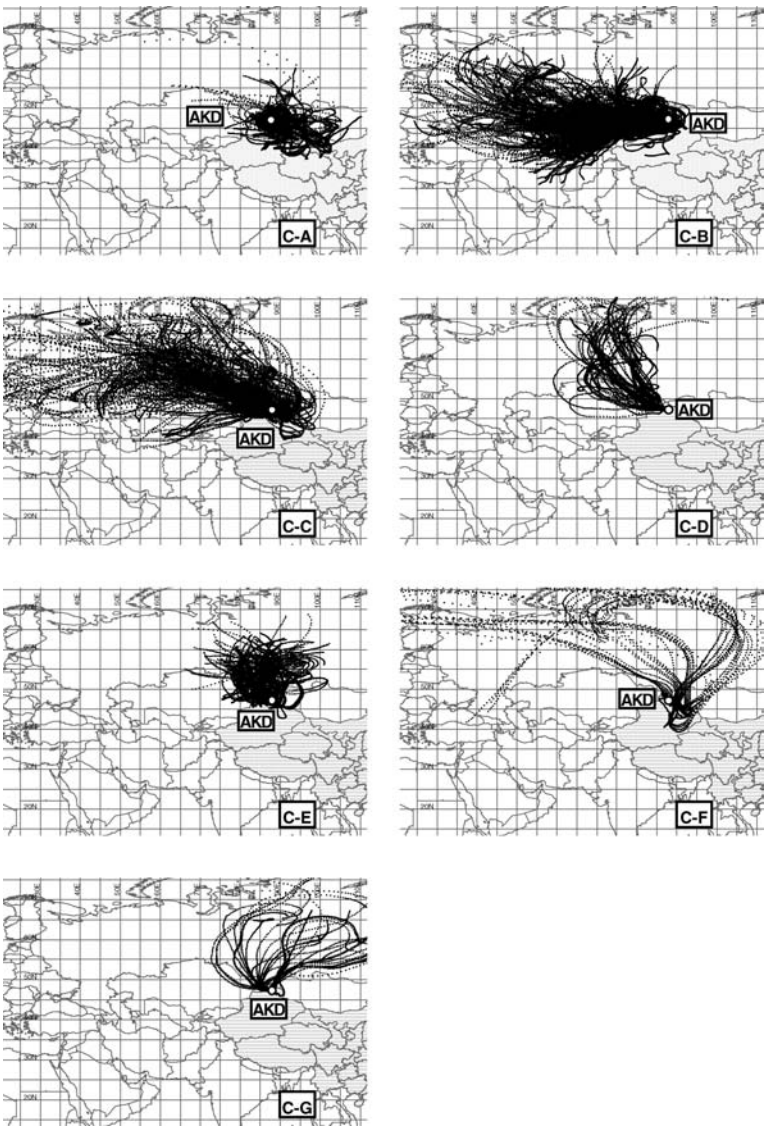

Fig. 11. Individual 5-d backwards-in-time trajectories for clusters A–G (C-A–G) terminating at AKD. The interval between the adjacent points for each trajectory is 1 hour. The shadowed area represents continental China.

industries include petroleum, coal and metallurgy. These implied pollution sources from Russian steel and coal industries may well impact the northern Xinjiang area, and as elsewhere, the effects of transboundary transport will complicate the development and implementation of pollution control strategies. The polluted C-A (southeasterly) trajectories passed over or near areas with extensive coal and metal mining operations on the boundary between northwestern China and Mongolia before arriving at AKD.

The second group of clusters followed a high-latitude northwesterly route to AKD, and they had lower concentrations of PM_{10}, OC, EC, SO_4^{2-}, NO_3^-, NH_4^+, K^+, Ca^{2+} and Mg^{2+} than the other groups. The C-F trajectories came from high latitude areas in eastern Europe and western Russia, and they mainly occurred in autumn. These trajectories covered comparatively long distances, and their mean height was ~3500 m: these are conditions that would favor the dispersion and dilution of pollutants. The C-D trajectories originated in the Russian high latitudes, and the loadings for most aerosol species for this group of trajectories were low indicating that this was another pathway for clean air.

The third group of clusters (C-B and C-C, westerly trajectories) accounted for 70% of all the trajectories to AKD, and they followed a similar path which was controlled by the prevailing westerly winds. Therefore, these trajectories probably delivered some dust from the deserts in eastern Kazakhstan. In addition, higher levels of OC, SO_4^{2-}, NO_3^- and NH_4^+ for the shorter distance C-B cluster compared with those for the long distance C-C pathway probably resulted from a stronger westerly transport of nearby anthropogenic pollutants. Clusters C-B and C-C had comparatively high levels of Ca^{2+} and Mg^{2+}, and the concentrations of Na^+, K^+ and F^- were quite similar among these

Table 6. Contribution percentage of each trajectory cluster and the corresponding mean concentrations of OC, EC, VOC, WS ionic species and selected trace elements in PM_{10} at ZUZ and AKD

	Proportion of all trajectories (%)				Mean concentration ($\mu g\ m^{-3}$)									Mean concentration ($ng\ m^{-3}$)					
ZUZ trajectory cluster	Aug	Autumn	Winter	Sum	OC	EC	VOC	$SO4^{2-}$	NO_3^+	NH_4+	K^+	Na^+	Ca^{2+}	S	K	Ca	Fe	Pb	As
2	38	10		10	**3.6**[a]	**0.38**	**0.63**	**2.0**	0.43	0.12	0.071	**0.74**	**0.64**	**309**	**48**	**138**	**46**	**5.4**(206[b])	**3.4**(1711)
3	18	3		3.9	**3.4**	**0.54**	**0.62**	**2.5**	0.39	0.33	0.090	**0.50**	**0.47**	**597**	**76**	**128**	**55**	**11**(359)	**3.5**(1489)
1	40	42	12	29	3.0	0.30	**0.36**	1.2	0.45	0.09	0.062	0.67	0.52	134	29	**112**	26	3.2(219)	2.0(1805)
4	4.0	17	16	15	2.8	0.30	0.19	**1.7**	0.45	0.15	0.082	0.67	0.38	181	46	**120**	**44**	2.8(112)	1.4(732)
5			10	4.2	**3.5**	**0.40**	0.07	1.5	**0.51**	**0.19**	**0.13**	**0.91**	0.46	181	**62**	72	**45**	1.8(71)	1.6(835)
6		21	56	33	3.0	**0.35**	0.18	**1.7**	**0.46**	**0.19**	**0.094**	0.64	0.43	193	**52**	80	**43**	2.6(104)	1.7(908)
7		7.1	6.1	5.7	**3.1**	0.34	0.30	1.4	0.38	0.11	0.070	0.62	0.43	134	43	95	36	3.0(145)	2.2(1417)
Total					3.1	0.34	0.31	1.6	0.45	0.15	0.082	0.68	0.49	205	46	105	39	3.9(177)	2.2(1294)

	Proportion of all trajectories (%)					Mean concentration ($\mu g\ m^{-3}$)								
AKD trajectory cluster	Jul–Aug	Autumn	Winter	Mar	Sum	OC	EC	VOC	$SO4^{2-}$	$NO3^-$	$NH4^+$	Mg^{2+}	Na^+	Ca^{2+}
A	12	4.4	8.6	17	8.9	2.9	**0.36**	0.48	**3.4**	**0.74**	**0.65**	0.044	**0.50**	0.53
E	16	4.4	13	3.2	9.6	**3.1**	**0.52**	0.38	**3.7**	0.53	**0.71**	**0.050**	**0.49**	0.46
G	2.0	1.9	6.1		3.1	**5.3**	**0.99**	**0.66**	**5.7**	**0.95**	**1.02**	**0.050**	0.46	0.58
D	14	4.1	1.9		5.1	2.7	0.30	0.41	2.5	0.43	0.45	0.035	0.38	0.21
F		11		1.6	3.8	2.1	0.14	0.35	1.9	0.47	0.26	0.028	0.39	0.44
B	43	44	57	39	48	**3.0**	0.32	**0.72**	**3.6**	**0.65**	**0.64**	**0.050**	**0.48**	**0.73**
C	14	29	13	40	22	2.3	0.24	0.38	3.0	0.50	0.49	**0.047**	**0.48**	**0.60**
Total						2.9	0.35	0.58	3.3	0.58	0.60	0.045	0.46	0.59

[a]Boldface indicated the values which were higher than the mean value of total samples; [b]EFcrust = (Element/Fe)air / (Element/Fe)crust, only EFcrust values larger than 5 were listed.

clusters, suggesting they may be affected by salinized dust from Gobi, sandy lands and deserts in the area.

Indeed, all of the AKD trajectory clusters, except those from the high latitudes (Clusters C-D and C-F), had similar concentrations of ions, including Ca^{2+}, Mg^{2+} and Na^{+}, that likely were derived from salinized soils or solonchaks (soils with salts contents greater than 0.3–0.5%, which form as salts accumulate in the pooly drained soils in arid and semi-arid area). This implies a relatively stable contribution of entrained dust to the WS ions in the aerosol particles. In arid regions, WS salts are known to accumulate on the surface of Gobi and sandy lands, and these can be injected into the atmosphere along with the dust and become an important component of the aerosols. Chemical analysis and surface structure analysis of the individual particles by X-ray photoelectron spectrometry have shown that the aerosol Na^{+}, Cl^{-} and SO_4^{2-} during dust storms in Beijing most likely originated from a salinized soil which was enriched with chloride and sulphate (Zhang et al., 2004).

The geographical distribution of the transport pathways showed that the air sampled at AKD most often arrived from the west and north-west. Therefore, the composition of the air at AKD arguably represents background atmospheric conditions in northern Xinjiang Province and neighboring areas. This regional background is strongly influenced by the transport of pollutants from countries upwind, making this site well suited for monitoring the transboundary influx of pollutants.

4. Conclusions

A formal or strict definition of 'aerosol background' in China has yet to be made to the authors' knowledge. A 'natural background', that is, one without detectable human influence (Hidy and Blanchard, 2005), is doubtlessly not measurable. On the other hand, the well-mixed aerosol at remote sites near the Chinese border, such as ADK and ZUZ, arguably represents a regional 'unmanageable background'. The low and relatively stable aerosol concentrations at ZUZ and AKD suggest that both sites sample air that generally represents regional background conditions.

We found that the mean OC and EC concentrations at the two sites were similar and comparable with those reported for global background sites. The fact that the aerosol composition at both sites was comparatively constant compared with more polluted sites presumably reflects mixing upwind and the dilution of pollutants during transport. Nevertheless, differences in the mass contributions from OC, sulphate, soil dust and EC to the aerosol populations at ZUZ and AKD do suggest some diversity in both natural and anthropogenic emissions as well as differences in regional pollutant transport to these remote areas in China.

Seasonal variations in the aerosol populations were more evident at AKD compared with ZUZ, and this probably reflects stronger pollutant impacts at AKD and more seasonality in the anthropogenic emissions upwind. Indeed, the aerosol populations at AKD appear to be more strongly influenced by seasonal changes in emissions than by variations in atmospheric transport. On the other hand, there were obvious seasonal variations in transport to ZUZ which can be explained by seasonal shifts in the atmospheric circulation affecting this low-latitude area.

According to Hidy and Blanchard (2005), the background characterization of atmospheric aerosols in a region is too complex to be represented only by average values. They suggested that using median values for the lower parts of the concentration distributions as well as the variation and frequency of these values derived from long-term and multi-sites observations are a better representation of background conditions. In fact, seasonal representations of relatively stable aerosol concentrations with occasional pulses from anthropogenic sources or rapid transport – as reported in this study – are likely the most meaningful way to operationally define an aerosol background. Taken in a broader context, we note that aerosol data available from remote sites in China are still quite limited and that global and regional emissions are continually changing; therefore establishing background conditions remains a significant challenge.

Finally, the combination of chemical data and meteorological analyses presented here strongly suggests that measurable quantities of air pollutants cross both the southwestern and the northwestern borders of China. Air from the southwest flows into China during the summer, and in winter, flow into China is often from the north-west. This transboundary influx of pollutants and its contribution to background conditions will need to be taken into account as air pollution control strategies for China are developed and implemented.

5. Acknowledgments

We are grateful to both anonymous reviewers for their constructive suggestions and comments. This research was supported by National Basic Research Program of China (Grant No. 2006CB403701, 2006CB403702) and by NSF ATM 0404944. Any opinions, findings and conclusions or recommendations expressed in this material are those of the authors and do not necessarily reflect the views of the sponsors. Thanks are also extended to Dr. Sun Junying who helped with the OC/EC measurements and to members of CAWAS at Chinese Academy of Meteorological Sciences for their support and many contributions to the project.

References

Arimoto, R., Snow, J. A., Graustein, W. C., Moody, J. L., Ray, B. J. and co-authors. 1999. Influences of atmospheric transport pathways on radionuclide activities in aerosol particles from over the North Atlantic. *J. Geophys. Res.Atmos.* **104**, 21301–21316.

Arimoto, R., Hogan, A., Grube, P., Davis, D., Webb, J. and co-authors. 2004a. Major ions and radionuclides in aerosol particles from the South Pole during ISCAT-2000. *Atmos. Environ.* **38**, 5473–5484.

Arimoto, R., Zhang, X. Y., Huebert, B. J., Kang, C. H., Savoie, D. L. and co-authors. 2004b. Chemical composition of atmospheric aerosols from Zhenbeitai, China, and Gosan, South Korea, during ACE-Asia. *J. Geophys. Res.Atmos.* **109**, D19S04, doi: 10.1029/2003JD004323.

Cao, G. L., Zhang, X. Y. and Zheng, F. C. 2006. Inventory of black carbon and organic carbon emissions from China. *Atmos. Environ.* **40**, 6516–26527.

Chow, J. C. and Watson, J. G. 2002. PM2.5 carbonate concentrations at regionally representative Interagency Monitoring of Protected Visual Environment sites. *J. Geophys. Res.Atmos.* **107**(D21), 8344, doi: 10.1029/2001JD000574.

Dai, S. G. 1997. *Environmental Chemistry*. Higher Education Press, Beijing, pp. 64–75. (in Chinese)

Draxler, R. R. and Hess, G. D. 1998. An overview of the HYSPLIT_4 modelling system for trajectories, dispersion, and deposition. *Aust. Meteorol. Mag.* **47**, 295–308.

Dusek, U. 2000. Secondary organic aerosol – Formation mechanisms and source contributions in Europe. (www.iiasa.ac.at) Interim Report IR-00-066. pp. 6.

Hidy, G. M. and Blanchard, C. L. 2005. The midlatitude North American background aerosol and global aerosol variation. *J. Air & Waste Manage. Assoc.* **55**, 1585–1599.

Hitzenberger, R. and Tohno, S. 2001. Comparison of black carbon (BC) aerosols in two urban areas—concentrations and size distributions. *Atmos. Environ.* **35**, 2153–2167.

Jain, M., Kulshrestha, U. C., Sarkar, A. K. and Parashar, D. C. 2000. Influence of crustal aerosols on wet deposition at urban and rural sites in India. *Atmos. Environ.* **34**, 5129–5137.

Kaufman, Y. J., Tanre, D. and Boucher, O. 2002. A satellite view of aerosols in the climate system. *Nature* **419**, 215–223.

Kim, Y. P., Moon, K. C., Shim, S. G., Lee, J. H., Kim, J. Y., and co-authors. 2000. Carbonaceous species in fine particles at the background sites in Korea between 1994 and 1999. *Atmos. Environ.* **34**, 5053–5060.

Krivácsy, Z. and Molnár, Á. 1998. Size distribution of ions in atmospheric aerosols. *Atmos. Res.* **46**, 271–291.

Ma, J. Z., Tang, J., Li, S. M. and Jacobson, M. Z. 2003. Size distributions of ionic aerosols measured at Waliguan Observatory: Implication for nitrate gas-to-particle transfer processes in the free troposphere. *J. Geophys. Res.-Atmos.* **108**(D17), 4541, doi: 10.1029/2002JD003356.

Moody, J. L. and Galloway, J. N. 1988. Quantifying the relationship between atmospheric transport and the chemical composition of precipitation on Bermuda. *Tellus* **40B**, 463–479.

Noguchi, I. and Hara, H. 2004. Ionic imbalance due to hydrogen carbonate from Asian dust. *Atmos. Environ.* **38**, 6969–6976.

Song, Y. L., Zheng, S. H., Liu, Y. J. and Zhang, Y. S. 2005. Research on characteristics of air pollution in Beijing during 2000–2002. *J. Appl. Meteorol. Sci.* **16**(suppl.), 116–122. (in Chinese)

Stohl, A. 1998. Computation, accuracy and applications of trajectories—a review and bibliography. *Atmos. Environ.* **32**, 947–966.

Taylor, S. R. and McLennan, S. M. 1995. The geochemical evolution of the continental crust. *Rev. Geophys.* **33**, 241–265.

Tang, J., Yu, X. L. and Xue, H. S. 2005. Observation of the water-soluble species in aerosols in summer in Lhasa area: Contribution of biomass burning emission. In: *The eighth symposium on aerosol research and aerosol technology in China and cross the Taiwan Strait*. pp. 355. (in Chinese)

Wang, T., Wong, C. H., Cheung, T. F., Blake, D. R., Arimoto R. and co-authors. 2004. Relationships of trace gases and aerosols and the emission characteristics at Lin'an, a rural site in eastern China, during spring 2001. *J. Geophys. Res.Atmos.* **109**, D19S05, doi: 10.1029/2003JD004119.

Xu, J., Bergin, M. H., Yu, X., Liu, G., Zhao, J. and co-authors. 2002. Measurement of aerosol chemical, physical and radiative properties in the Yangtze delta region of China. *Atmos. Environ.* **36**, 161–173.

Xu, J., Bergin, M. H., Greenwald, R. and Russell, P. B. 2003. Direct aerosol radiative forcing in the Yangtze delta region of China: Observation and model estimation. *J. Geophys. Res.Atmos.* **108**(D2), 4060, doi: 10.1029/2002JD002550.

Zhang, X. Y., Arimoto, R., An, Z. S., Chen, T., Zhang, G. Y. and co-authors. 1993. Atmospheric trace elements over source regions for Chinese dust: Concentrations, sources and atmospheric deposition on the Loess Plateau. *Atmos. Environ.* **27A**, 2051–2067.

Zhang, X. Y., Cao, J. J., Li, L. M., Arimoto, R., Cheng, Y. and co-authors. 2002. Characterization of atmospheric aerosol over XiAn in the South Margin of the Loess Plateau, China. *Atmos. Environ.* **36**, 4189–4199.

Zhang, X. Y., Gong, S. L., Zhao, T. L., Arimoto, R., Wang, Y. Q. and co-authors. 2003a. Sources of Asian dust and role of climate change versus desertification in Asian dust emission. *Geophys. Res. Lett.* **30**(24), 2272, doi: 10.1029/2003GL018206.

Zhang, X. Y., Gong, S. L., Arimoto, R., Shen, Z. X., Mei, F. M. and co-authors. 2003b. Characterization and temporal variation of Asian dust aerosol from a site in the northern Chinese deserts. *J. Atmos. Chem.* **44**, 241–257.

Zhang, X. Y., Wang, Y. Q., Wang, D., Gong, S. L., Arimoto, R. and co-authors. 2005. Characterization and sources of regional-scale transported carbonaceous and dust aerosols from different pathways in coastal and sandy land areas of China. *J. Geophys. Res.Atmos.* **110**, D15301, doi: 10.1029/2004JD005457.

Zhang, X. Y., Zhuang, G. S. and Yuan, H. 2004. The dried salt-lakes saline soils sources of the dust storm in Beijing: The individual particles analysis and XPS surface structure analysis. *China Environ. Sci.* **24**, 533–537. (in Chinese)